Articles

Differences in Binding Specificity for the Homologous γ- and β-Chain "Holes" on Fibrinogen: Exclusive Binding of Ala-His-Arg-Pro-amide by the β-Chain Hole[†,‡]

Russell F. Doolittle,* Albert Chen,[§] and Leela Pandi

Department of Chemistry and Biochemistry and Division of Biology, University of California at San Diego, La Jolla, California 92093-0314

Received June 19, 2006; Revised Manuscript Received September 21, 2006

ABSTRACT: The β-chain amino-terminal sequences of all known mammalian fibrins begin with the sequence Gly-His-Arg-Pro- (GHRP-), but the homologous sequence in chicken fibrin begins with the sequence Ala-His-Arg-Pro- (AHRP-). Nonetheless, chicken fibrinogen binds the synthetic peptide GHRPam, and a previously reported crystal structure has revealed that the binding is in exact conformance with that observed for the human GHRPam−fragment D complex. We now report that human fibrinogen, which is known not to bind APRP, binds the synthetic peptide AHRPam. Moreover, a crystal structure of AHRPam complexed with fragment D from human fibrinogen shows that AHRPam binds exclusively to the β-chain hole and, unlike GHRPam, not at all to the homologous γ-chain hole. The difference can be attributed to the methyl group of the alanine residue clashing with a critical carboxyl group in the γC hole but being accommodated in the roomier βC hole where the equivalent carboxyl is situated more flexibly.

In vertebrates, fibrinogen is transformed into a fibrin clot by the thrombin-catalyzed removal of peptide material from the amino-terminal segments of the α- and β-chains (*1*). The release of these peptides, fibrinopeptides A and B, exposes two sets of "knobs", A and B, which fit into complementary "holes" on neighboring molecules (*2*). Typically, A-knobs begin with the sequence Gly-Pro-Arg- and B-knobs with the sequence Gly-His-Arg-, although in some nonmammalian vertebrates differences have been observed.

Synthetic peptides corresponding to A-knobs bind to fibrinogen and prevent polymerization (*3*, *4*). Synthetic B-knobs bind to fibrinogen but, under most conditions, do not inhibit fibrin formation (*3*−*5*). Instead, the binding of synthetic B-knobs leads to more turbid clots (*3*, *6*), the apparent result of enhanced lateral association of the polymerizing protofibrils. Although numerous factors can affect the turbidity of clots, which in the extreme are denoted as "fine" or "coarse" (*7*), synthetic B-knobs are unique in that the enhanced turbidity is accompanied by resistance to fibrinolysis and a delay in the fibrin-catalyzed activation of tPA[1] (*8*).

When both synthetic A- and B-knobs are present in a solution of fibrinogen or fragment D or D-dimer, invariably the two peptides each find their respective holes, their different structures being readily distinguished (*9*, *10*). The architectures of the two homologous holes are remarkably similar, however, and it has not been immediately obvious how the sites discriminate between the two ligands. If only one of the synthetic knobs is present, it will bind to both kinds of hole (*3*, *4*).

An opportunity for investigating specific differences arose when it was found that the β-chain of chicken fibrin has an amino-terminal alanine instead of glycine (*11*). The finding was unexpected because it had been previously demonstrated that human fibrinogen does not bind the synthetic peptide APRP or other non-glycyl peptides (*4*), and it was presumed the requirement for amino-terminal glycine extended to the B-knob also. Fortuitously, chicken fibrinogen bound the previously synthesized peptide GHRPam, and a crystal structure at 2.7 Å resolution showed it bound to the β-chain holes in the same way as in fragments D and D-dimer from human fibrinogen (*12*).

The existence of amino-terminal alanine in the chicken fibrin β-chain suggested that the βC hole was a more promiscuous binder than the γC hole. As such, we examined the influence of the synthetic peptide AHRPam on the

[†] This work was supported in part by grants from the National Heart, Lung and Blood Institute (HL-81553) and the American Heart Association.

[‡] The atomic coordinates and structure factors for FDAH have been deposited in the Protein Data Bank as entry 2H43.

* To whom correspondence should be addressed. Telephone: (858) 534-4417. Fax: (858) 534-4985. E-mail: rdoolittle@ucsd.edu.

[§] Present address: Baylor College of Medicine, Houston, TX 77030.

[1] Abbreviations: AHRPam, Ala-His-Arg-Pro-amide; GHRPam, Gly-His-Arg-Pro-amide; dAPRPam, D-Ala-Pro-Arg-Pro-amide; AHRPY, Ala-His-Arg-Pro-Tyr-amide; GHRPYam, Gly-His-Arg-Pro-Tyr-amide; FDAH, fragment D complexed with AHRPam; FDGH, fragment D complexed with GHRPam; DDGH, D-dimer complexed with GHRPam; DDBO, D-dimer complexed with GPRPam and GHRPam; DDNL, D-dimer with no ligands; PEG, polyethylene glycol; MPD, methylpentanediol; tPA, tissue plasminogen activator.

10.1021/bi061219e CCC: $33.50
Published on Web 11/02/2006

formation of human fibrin. In fact, the alanyl peptide enhances the turbidity of fibrin clots prepared from human fibrinogen in the very same way that GHRPam does. Accordingly, we prepared crystals of fragment D from human fibrinogen in the presence of the synthetic peptide AHRPam and determined a structure by X-ray crystallography. We have found that, unlike the synthetic peptide GHRPam, AHRPam binds exclusively to the β-chain hole. The presence or absence of ligand was verified not only by the presence or absence of electron density in suitably calculated omit maps but also by the conformations of key residues known to move as a result of ligand binding.

We also conducted experiments on fibrin formation with the corresponding L-alanine analogue of the A-knob, APRPam, and confirmed that it does not have a significant effect on fibrin formation (human). A report (*13*) that D-alanine can replace glycine in these peptides (dAPRP) and can prevent fibrin formation could not be confirmed, no inhibition of thrombin-induced clotting or reassociation of fibrin monomers being observed with human fibrinogen in the presence of that synthetic peptide.

The question of how the β-chain hole is able to accommodate an alanyl peptide while the γ-chain hole cannot was addressed by comparing the new structure with numerous previously reported structures of fragment D and D-dimer complexed with various combinations of peptides. In the end, it was possible to pinpoint particular features that make the γ-chain hole more discriminating.

MATERIALS AND METHODS

The synthetic peptides Ala-His-Arg-Pro-amide, Ala-His-Arg-Pro-Tyr-amide, Ala-Pro-Arg-Pro-amide, and D-Ala-Pro-Arg-Pro-amide were purchased from Sigma-Genosys. The peptides Gly-His-Arg-Pro-amide and Gly-Pro-Arg-Pro-amide were those described in earlier publications from this laboratory (*9*, *12*, *14*−*16*) and had been synthesized by the BOC procedure (*17*). Fibrinogen was prepared from human blood plasma as described previously; protocols for the purification of fragments D and D-dimer have also been fully described in previous publications (*9*, *12*, *14*−*16*). Human thrombin was purchased from Enzyme Research Corp. Fibrin monomer reassociation assays (*18*) were conducted by diluting 50 μL of NaBr-dispersed human fibrin with 1.0 mL of 0.08 M phosphate buffer (pH 6.8) containing various peptide additives, and following the resulting turbidity in a spectrophotometer at 350 nm (λ). The details of this assay and others involving thrombin−fibrinogen and thrombin−tPA−fibrinogen species have been described in a recent publication (*8*).

Crystals were obtained by vapor diffusion from sitting drops at room temperature. Crystals of the fragment D−AHRPam complex were grown from drops containing equal volumes of a 10 mg/mL protein solution in 0.05 M Tris (pH 7.0), 5 mM $CaCl_2$, containing 8 mM AHRPam, and a well solution composed of 0.05 M Tris (pH 8.0) containing 15% PEG-3350, 10 mM $CaCl_2$, and 2 mM sodium azide. The final (pre-equilibration) concentration of calcium in the drop was 7.5 mM. Cryoprotection before crystals were frozen was achieved by gradually adding MPD to a final concentration of 15%.

Preliminary screening of crystals was performed at the University of California at San Diego X-ray Crystallography Facility. Full sets of diffraction data were collected at beamline 5.0.1, the Advanced Light Source, Lawrence Berkeley National Laboratory (Berkeley, CA). Data were processed with HKL2000 (at the Advanced Light Source) and with Denzo and Scalepack (*19*). The structure was determined by molecular replacement with Amore (*20*). Refinement was accomplished with CNS (*21*), R_{free} being used as a guide to rebuilding throughout; rebuilding depended heavily on O (*22*).

Model Comparisons. Numerous comparisons with previously reported structures of fragments D and D-dimer were conducted in an effort to identify any features of the β- and γ-chain holes that might be responsible for differences in discrimination. Structures were downloaded from the Protein Data Bank (*23*) or were the results of our own studies. These included crystallographic models with either GPRPam (or in one case GPRP) or GHRPam bound to one hole, the other hole, neither, or both. Special attention was paid to the conformational changes that occur when the various peptides are bound. Although the models varied with regard to their final resolution and had small discrepancies that were likely due to differences in data processing, model building, and protocols used for refinement, a consistent pattern of knob−hole interactions and attendant conformational change was readily established.

For the most part, comparisons were limited to the 90- or 94-residue domains that contain the knob-binding pockets, and the synthetic knobs bound by them. Model comparisons were made after all structures were superimposed onto a common reference point with O (*22*). Various distance measuring programs contained in the original XPLOR package (*24*) or in CCP4 (*20*) were employed to determine all distances of $\leq$4.0 Å between every non-hydrogen knob atom and the host protein. Some other distances between key atoms were determined directly from PDB coordinate files by use of a perl script in conjunction with Excel (we are grateful to J. Nand for writing this script). Illustrations were prepared with the aid of PyMol (*25*).

Because the emphasis is entirely on structures derived from fragments D and D-dimer from human fibrin(ogen), comparisons with and references to structures from chicken and lamprey fibrin(ogen) always employ numbering corresponding to the human structures. Sequence comparisons for the various knobs and holes are provided as Supporting Information (Figures S1 and S2).

RESULTS

Effect of Alanyl Peptides on Human Fibrin Formation. When human fibrinogen is clotted in the presence of AHRPam, the enhancement of turbidity is similar to that observed with GHRPam (Figure 1A). In contrast, the corresponding alanine analogue of the A-knob is without effect, neither enhancing nor inhibiting fibrin formation (Figure 2A). Similarly, the D-alanine peptide was also without effect (Figure 2A). Equivalent results were obtained with the reassociation of fibrin monomers in the presence of these peptides, confirming that the enhancement is independent of thrombin activity (Figures 1B and 2B).

Alanyl B-knobs were also effective in delaying fibrinolysis. As in the case of glycine-ending B-knobs (*8*), a pentapeptide with a carboxy-terminal tyrosine is considerably

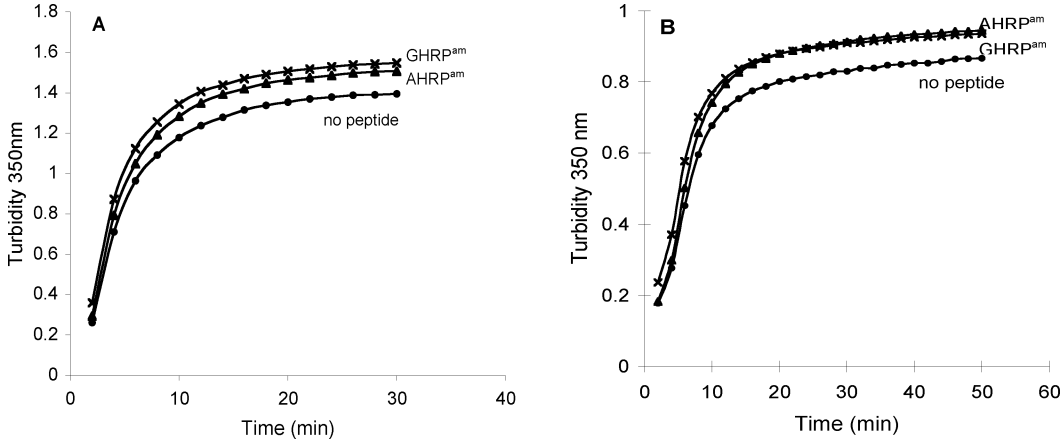

FIGURE 1: Synthetic B-knobs with amino-terminal alanine enhance the turbidity of clots formed from human fibrinogen, whether generated directly by thrombin (A) or by the reassociation of fibrin monomers (B). (A) Thrombin-generated fibrin in the presence of 200 μM AHRPam (▲), 200 μM GHRPam (×), or no peptide (control) (●). The initial concentration of fibrinogen was 3.3 μM. (B) Reassociation of fibrin monomers in presence of 200 μM AHRPam (▲), 200 μM GHRPam (×), or no peptide (control) (●). Turbidity was measured at 350 nm (λ).

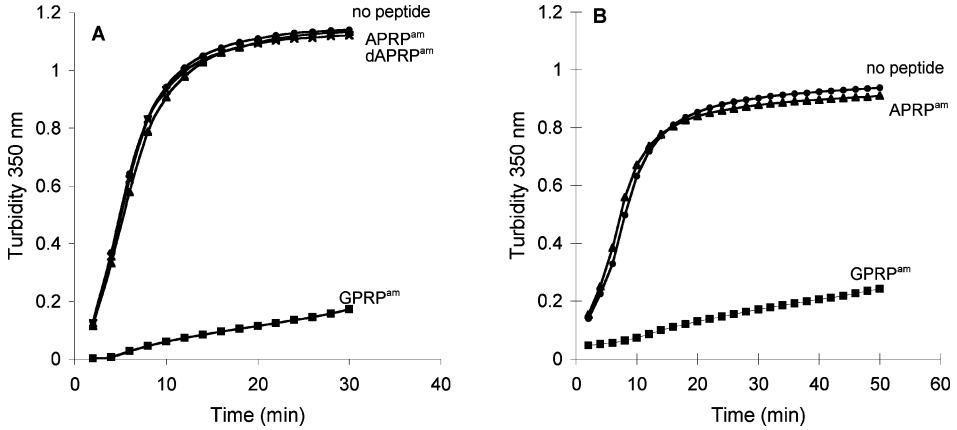

FIGURE 2: Synthetic fibrin A-knobs with amino-terminal alanine do not inhibit formation of fibrin from human fibrinogen, whether generated directly by thrombin (A) or by the reassociation of fibrin monomers (B). (A) Thrombin-generated fibrin in the presence of 0.5 mM GPRPam (■), 2.0 mM APRPam (◆), 2.0 mM dAPRPam (×), or no peptide (control) (●). (B) Reassociation of fibrin monomers in the presence of 0.5 mM GPRPam (■), 2.0 mM APRPam, (◆), or no peptide (control) (●). The concentration of fibrin monomer after dilution was 0.65 mg/mL (2.0 μM). Turbidity was measured at 350 nm (λ).

more effective than the tetrapeptide. The peptide AHRPYam is only slightly less effective than GHRPYam in delaying the fibrin-catalyzed activation of plasminogen by tPA (Figure 3).

Crystal Structure of Fragment D Complexed with AHRPam. The structure of fragment D from human fibrinogen complexed with the synthetic peptide AHRPam was determined at 2.7 Å (Table 1). In contrast to crystals of the same material complexed with GHRPam (*16*), the space group and unit cell are virtually the same as those of fragment D crystals prepared without any peptide ligand (*14*−*16*).

It was found that AHRPam is restricted to the β-chain holes and is absent from the γ-chain holes. These judgments were made initially on the basis of electron density in $|F_o| - |F_c|$ omit maps (Figure 4) and then confirmed by noting the conformations of key residues that are parts of the two different binding sites (Figure 5A,B). Most relevant were direct comparisons with the previously reported structures of fragments D (FDGH, PDB entry 1FZG) and D-dimer (DDGH, PDB entry 1FZF) complexed with GHRPam (*16*).

The most obvious difference between the GHRP and AHRP complexes is the absence of electron density from the γC holes of FDAH and its presence in the γC holes in FDGH and DDGH (*16*). Beyond that, the side chain orientations of γTyr363 are very different in the AHRPam and GHRPam structures, in accord with previous observations about occupancy of the γ-chain site (Figure 5A). Additionally, there are significant differences in the adjacent loop formed by residues γ358−362. Finally, the secondary calcium site involving γ-chain residues Asp294, Gly296, Asp298, and Asp301 that was found for FDGH when the γC hole is occupied by GHRPam (*16*) is not found in FDAH. All of these observations are in accord with the ligand AHRPam not being bound by the γ-chain hole.

In the case of the βC domains, however, there are virtually no differences between the new structure with bound AHRPam and the previously reported ones with GHRPam, the AHRPam ligand being clearly present in both βC holes in FDAH (Figure 4). Moreover, residues βGlu397 and βAsp398 are positioned in the conformation found to correspond to ligand binding (Figure 5B). The rms fit (α-carbons only) for the full 94-residue length of the two β-hole domains is 0.368. In contrast, the rms fit for the corresponding 90-residue stretch of the γ-hole domains is 0.764. If the comparison is limited to the first 65 residues of the γ-chain, however, the rms fit drops to 0.492, in line with the

Table 1: Data Collection and Refinement Statistics for FDAH

space group	$P2_1$
unit cell dimensions	
a (Å)	105.0
b (Å)	47.9
c (Å)	171.4
β (deg)	105.4
no. of molecules per asymmetric unit	2
no. of observations	142342
highest resolution	2.7 (2.80−2.70)[a]
no. of unique reflections	42201 (2868)[a]
completeness (%)	91.9 (63.3)[a]
R_{sym} (I)[b]	0.074 (0.414)[a]
mean I/σ	8.5 (2.3)[a]
mosaicity (deg)	0.7
refinement resolution range (Å)	30−2.7
no. of residues in the protein	734
no. of residues in the model	662
no. of atoms in the model[c]	10776
average *B* factor (Å^2)	62.5
R-factor[d]	0.246
R_{free}[e]	0.299
rmsd for ideal bond lengths (Å)	0.008
rmsd for bond angles (deg)	1.44

[a] Values in parentheses describe the highest-resolution shell. [b] $R_{sym} = (\sum|I - \langle I\rangle|)/(\sum|I|)$. [c] Includes sugars and calcium atoms. [d] Crystallographic *R*-factor $[(\sum||F_o| - |F_c||)/(\sum|F_o|)]$ with 95% of the native data. [e] R_{free} is the *R*-factor based on 5% of the native data withheld from the refinement.

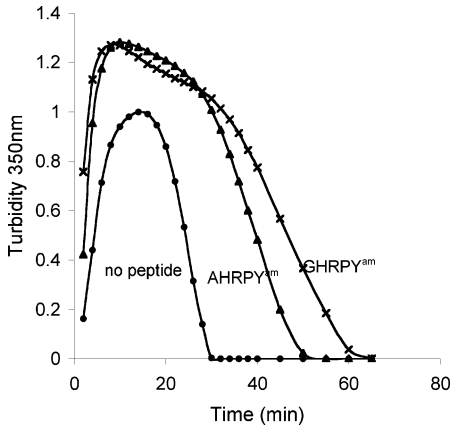

FIGURE 3: Synthetic B-knobs with amino-terminal alanine inhibit the fibrin-stimulated tPA activation of plasminogen in the same way as glycyl B-knobs. The concentration of human fibrinogen at time zero was 3.3 μM. A mix of thrombin and tPA was added such that their final concentrations were 0.08 and 0.29 μg/mL, respectively. The effect of added AHRPYam (▲) is compared with that of GHRPYam (×), both at final concentrations of 200 μM; control means no peptide (●).

observation that there is a major conformational difference in the terminal one-third of the sequence where loop III and γTyr363 exist. Finally, just as in the GHRPam structures (*16*), the calcium ion between the βC domain and coiled coil of FDAH persists with only three host protein ligands after the conformational change (Figure S3).

Excluding Alanyl Peptides from the γC Hole. Given how similar the βC and γC holes are, the question of how a γC hole can exclude an alanine-ending peptide while a βC hole does not arises. We approached the problem by examining previously published models of fragments D and D-dimer, some of which had their γC and βC holes occupied by GPRPam or GHRPam, and some not. To begin, we detailed the occurrence of each of the 12 hydrogen bonds that occur with both ligands and the host protein, and two others that involve bridging with a water molecule (Figures S4 and S5).

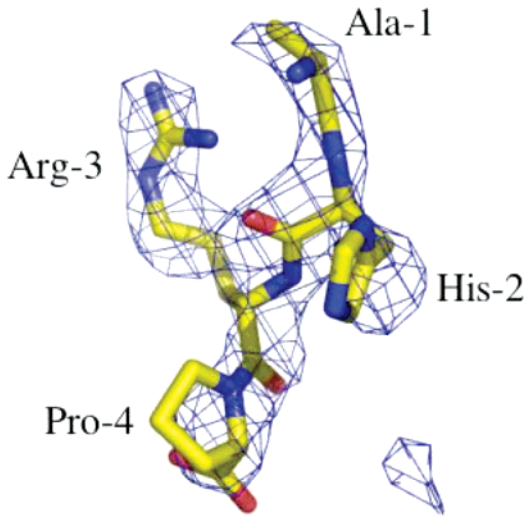

FIGURE 4: Electron density corresponding to AHRPam in the βC hole of fragment D (from human fibrinogen) as observed in an $|F_o| - |F_c|$ map calculated at 2.7 Å resolution and contoured at 3.0 σ. The peptide was not included in the calculation.

We also examined hydrophobic interactions that occur between the ligand and host protein in the two situations (Table S1). In both cases, aromatic residues pack against the backbone of arginine 3 of the ligand, γPhe322 in the γ-chain, and βTrp385 in the β-chain. In either situation, a minimum of six hydrogen−carbon bonds become shielded from solvent; this amounts to a free energy difference of ~20 kJ/mol (*27*). Also, in the γ-chain case, γPhe295 packs against the side chain of proline 2, another half-dozen hydrogen−carbon bonds being similarly excluded from contact with solvent. In the case of the β-chain, βLeu360 and βMet367 pack against the side chain of the histidine at ligand position 2. Clearly, nonpolar interactions contribute greatly to the binding of both peptide ligands.

As for the polar interactions, one set of hydrogen bonds stands at the heart of binding both peptides. Invariably, four hydrogen bonds occur between the ligand polypeptide backbone and a conserved three-residue backbone ridge in the host protein composed of residues that occur, in a sequence sense, between loop regions II and III. In the γ-chain, the key sequence (human) is Lys-Cys-His (residues γ338−340); in the β-chain, the sequence is Arg-Cys-His (residues β406−408). In both cases, an unusual cis peptide bond between Lys/Arg and Cys is what allows the Cys backbone nitrogen to participate in the process. In both holes, the canyon floors are marked by a ridge of these backbone atoms (shown as a line of red and blue spheres in Figure 6A,B). We used this fixed feature as a reference line for demonstrating the mobility of nearby groups, particularly the carboxyl group of γAsp364 or βAsp432.

Conformational Changes. Although it was apparent from the very first published structure of a γC domain that the binding pocket is composed of three extended loops (*28*), subsequent structures crystallized with synthetic peptide ligands showed that neither the γ-chain nor the β-chain binding sites are completely formed until after the peptide is bound. Interestingly, the conformational changes that occur involve different loops in the two different holes (*16*). Thus, in the case of the γ-chain hole, γTyr363, which resides in loop III, is known to shift its position when the hole is

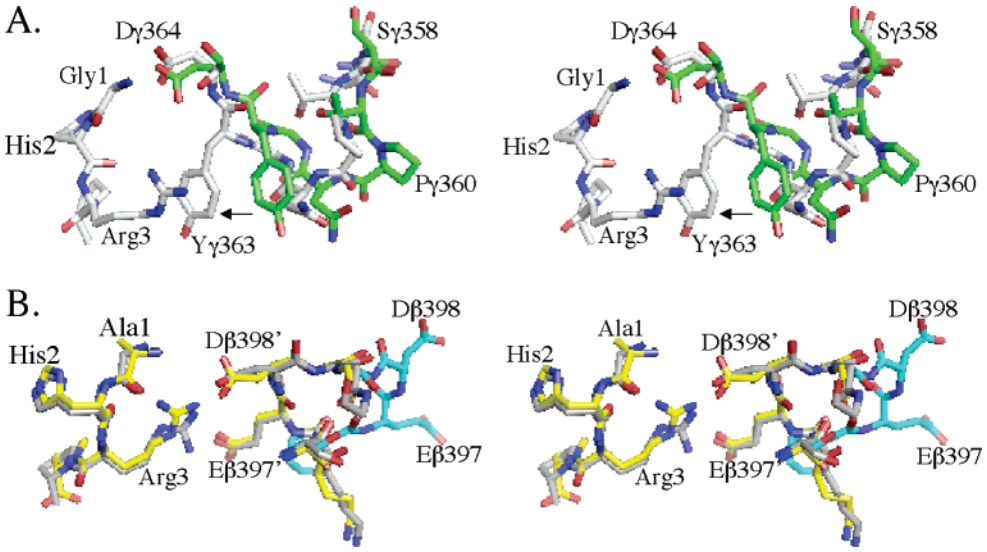

FIGURE 5: (A) Stereodiagram of γ-chain residues 357−364 from FDAH (green) and FDGH (white, PDB entry 1FZG) showing how the side chain of γTyr363 (yellow) shifts to interact with the guanidino group of the arginine at position 3 of the GHRPam ligand (also white, PDB entry 1FZG). The position of γTyr363 in FDAH confirms the absence of a ligand in its γC hole. (B) Stereodiagram of β-chain residues 396−401 from FDAH (yellow) and FDGH (also yellow, PDB entry 1FZG) with DDNL (green, PDB entry 1FZE), which is in the "unoccupied hole" conformation.

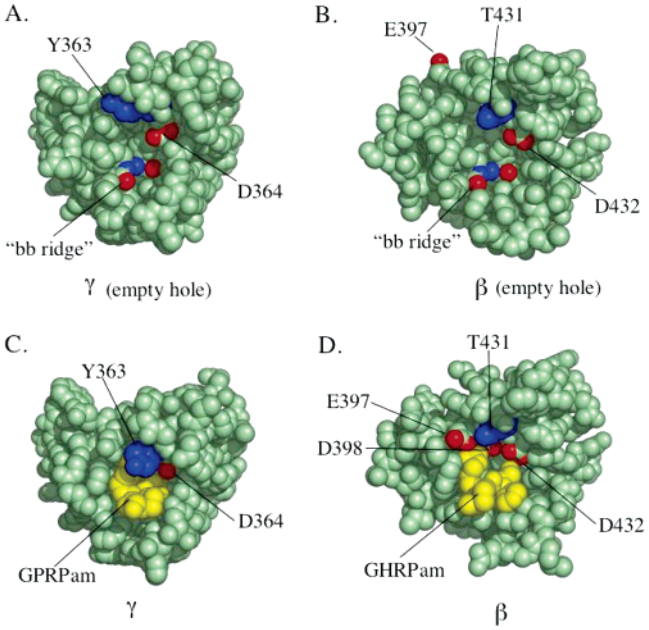

FIGURE 6: (A) Unoccupied hole in the γ-chain. The blue and red spheres in the hole are the nitrogen and oxygen atoms, respectively, in the backbone ridge ("bb ridge") provided by residues 338−340 (Lys, Cys, and His, respectively). (B) Unoccupied hole in the β-chain showing the same atoms in the corresponding bb ridge (residues 406−408, Arg, Cys, and His, respectively). (C) γ-Chain with its hole occupied by the peptide GPRPam (PDB entry 1FZC). Note the shift in the position of γY363 compared with its position in panel A. (D) β-Chain with its hole occupied by the synthetic peptide GHRPam (PDB entry 1FZC). Note the shift of βE397 (red) compared with its location in panel B.

occupied (Figure 5A) (*15*, *26*), whereas the corresponding residue in the β-chain, βT431, hardly moves during the transition from empty to occupied. Instead, the formation of the completed β-chain hole involves a radical change in loop II, residues βGlu397 and βAsp398 moving through an arc of 180° spanning 20 Å (Figure 5B). In this case, the corresponding residues in the γ-chain, residues γGln329 and γAsp330, are already in position in the unoccupied hole.

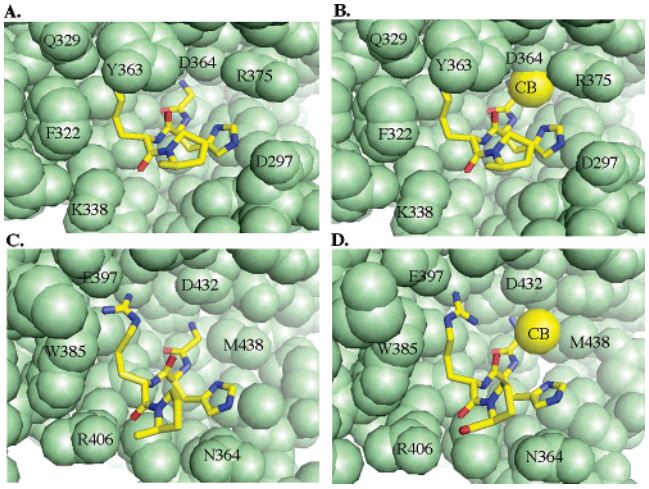

FIGURE 7: (A) Close-up view of the γ-chain hole (light green spheres) with peptide ligand GHRPam (yellow sticks) (PDB entry 1FZF). (B) Same structure with Gly1 of the peptide mutated in silico to alanine. The alanine CB is shown as a yellow sphere. (C) Close-up view of the β-chain hole (light green spheres) with peptide ligand GHRPam (yellow sticks) (PDB entry 1FZF). (D) Actual structure of the same region of fragment D crystallized with AHRPam (this study) (CB of alanine is shown as a yellow sphere).

Loop I (residues γ290−304 or β354−367) remains relatively fixed in both holes during the binding process.

General Hole Comparisons. Even at a gross level, casual inspection shows the β-chain hole to be more open and exposed than its γ-chain counterpart (Figure 6A,B). Moreover, the relative openness of the β-chain hole is evident even when the holes are filled (Figure 6C,D). The γ-chain hole is much better defined and closed off when occupied.

A Particular Difference. As a first step in pinpointing the differences that influence the binding of the peptide AHRPam, we changed the amino-terminal glycine residues of specified knobs in various published structures to alanine in silico. When this exercise was conducted with a structure in which the γ-chain hole is occupied by a the synthetic peptide GHRPam (PDB entry 1FZF or 1FZG), clashing

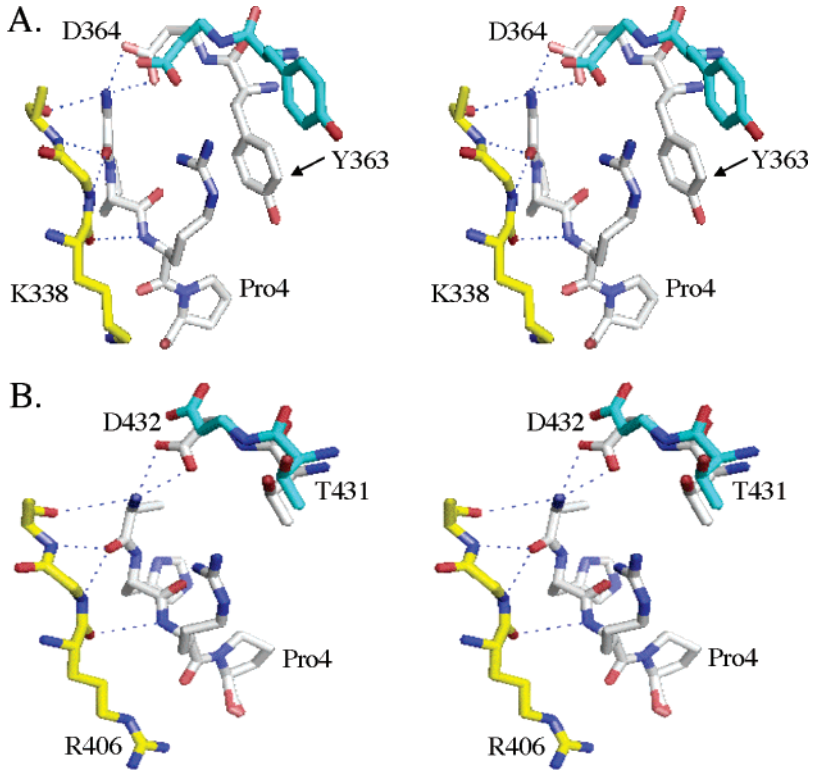

FIGURE 8: (A) Stereodepiction of the γ-chain backbone ridge (γK338-γC339-γH340, yellow), GPRPam peptide ligand (white), and residues γ363 and γ364 from DDBO (white, PDB entry 1FZC) compared with residues γ363 and γ364 from FDAH (green, this paper, PDB entry 2H43) after superposition of the two backbone ridges. Dotted lines show hydrogen bonds between backbone atoms and the ligand in DDBO. The side chain of γTyr363 from FDAH is in the unoccupied hole position. (B) Stereodepiction of the same view for the β-chain of the backbone ridge (βR406-βC407-βH408, yellow), AHRPam (white), and residues β431 and β432 from FDAH (white) compared with residues β431 and β432 of DDNL (green, PDB entry 1FZE) after superposition of two backbone ridges. Dotted lines show hydrogen bonds between backbone atoms and the ligand in FDAH.

occurs between the artificially introduced alanine CB atom and the carboxylate of a nearby aspartyl side chain (γAsp364), an entity that ordinarily interacts with the α-amino group of the peptide ligand (Figures 7A and S6A). When the same operation is performed with the same ligand in the β-chain hole, however, clashing with the corresponding aspartic carboxylate (βAsp432) does not occur (Figures 7B and S6B). The location of the alanine residue in the newly determined structure of fragment D complexed with AHRPam is virtually the same as that with FDGH (Figures 7D and S7).

As it happens, the side chains of both the γ- and β-chain aspartic acids (γAsp364 and βAsp432) shift measurably between the unoccupied and occupied forms, although more in the case of the β-chain than the γ-chain (Figures 8A,B and S8A,B). Moreover, the shift of γAsp364 is coupled with the previously mentioned movement of the adjacent tyrosine residue (γTyr363), the aromatic side chain of which becomes engaged in an interaction with the guanidino group of arginine 3 of the peptide. The comparable situation in the β-chain involves a threonine (βThr431), the movement of which appears to be without consequence. This difference, Tyr-Asp as opposed to Thr-Asp, involving as it does an important stabilizing interaction (*29*), appears to be critical in the distinction of γ- and β-chain holes. As a consequence, the clashing of the in silico-engineered alanine with γAsp364 leads to more than the loss of two hydrogen bonds, the concomitant tyrosyl shift not being able to occur either.

It should be noted that in the unoccupied situation, the carboxyl group of γAsp364 is hydrogen-bonded to the guanidino group of γArg375 (Figure S8A), the interaction being lost upon binding of the carboxylate to the glycine amino group of the ligand. In the β-chain, the situation is slightly different (Figure S8B). In the unoccupied situation, the carboxyl group of βAsp432 is hydrogen-bonded to βSer443 [which aligns with γArg375 by sequence (Figure S2)] and βTyr442. These interactions account for the pivotal

Table 2: Distances (angstroms) between Ridge Backbone Atoms[a] and Pivotal Aspartic Carboxylate[a] in Occupied and Unoccupied βC and γC Holes[b]

		mean *D* (standard deviation)			
	N[c]	Asp−O_{His}	Asp−N_{His}	Asp−N_{Cys}	Asp−$O_{Lys-Arg}$
HDγ empty	7	6.04 (0.73)	6.88 (0.37)	8.16 (0.94)	8.56 (0.27)
HDγ−GPRPam	7	5.48 (0.46)	6.88 (0.20)	8.34 (0.79)	9.03 (0.41)
change[d]		−0.52	0.00	+0.18	+0.47
HDβ empty	8	7.22 (1.09)	8.58 (1.03)	10.82 (1.31)	10.98 (1.05)
HDβ−GHRPam	8	5.78 (0.45)	6.79 (0.20)	7.84 (0.42)	9.08 (0.41)
change[d]		**−1.44**	**−1.79**	**−2.98**	**+1.90**
HDβ empty	8	7.22 (1.09)	8.58 (1.03)	10.82 (1.31)	10.98 (1.05)
HDγ empty	7	6.04 (0.73)	6.88 (0.37)	8.16 (0.94)	8.56 (0.27)
change[d]		**−1.18**	**−1.70**	**−2.66**	**−2.42**
HDβ−HRPam	8	5.78 (0.45)	6.79 (0.20)	7.84 (0.42)	9.08 (0.41)
HDγ−GHRPam	7	5.48 (0.46)	6.88 (0.20)	8.34 (0.79)	9.03 (0.41)
change[d]		−0.30	+0.09	+0.50	−0.05

[a] The host backbone residues are β406−408 and γ338−340; the aspartic residues are βAsp432 and γAsp364. The distances between the two carboxyl oxygen atoms and the four target atoms were averaged. [b] HD, human fragment D or D-dimer. [c] *N* is the number of "hole situations" examined. Based on PDB entries 1FIB, 2FIB, 1FZA, 1FZB, 1FZC, 1FZE, 1FZF, 1FZG, 1LT9, and 1LTJ, most of which have two sets of β- and γ-holes per structure. [d] The change is the difference in distances (angstroms) between empty and occupied holes or between β- and γ-holes. Statistically significant differences are shown in bold.

carboxyl group being held away from the backbone ridge in the absence of ligand.

In support of the notion that the clash of the alanyl CB with carboxylate of γAsp364 is what prohibits binding, we examined a dozen fragment D and D-dimer models with regard to the distances between key atoms in the highly conserved backbone ridge (Lys-Cys-His in the γ-chain and Arg-Cys-His in the β-chain) and the pivotal aspartic acid carboxylates (γAsp364 and βAsp432) (Table 2). A number of significant differences emerged. First, it is clear that in the β-chain the distances between these key atoms are greater in the unoccupied holes than they are after the ligand is bound (Table 2), a significant adjustment occurring that some might call an "induced fit" (*30*). Second, even though the β- and γ-holes are homologous and use equivalent residues in all their polar interactions with the peptide knobs, by these measures the unoccupied βC hole is significantly more expansive at its base than the γC hole (Table 2). Third, after the glycine-ending knobs are bound to their appropriate holes (i.e., GPRPam in the γC hole and GHRPam in the βC hole), the distances between the specified atoms in the two kinds of hole are approximately the same (Table 2). Thus, although the two holes end up with very similar arrangements of side chains, the β-hole starts out significantly looser and larger.

DISCUSSION

That the synthetic peptides GHRPam and AHRPam both enhance the turbidity of fibrin clots suggested a priori that the interaction involved the βC holes (*8*) and that this hole is a more promiscuous binder than the one in the γC domain. Just as early observations made it clear that the peptide APRP does not bind to human fibrinogen (*3*, *4*), neither does APRPam or dAPRPam affect fibrin formation in any way. These results are consistent with the fact that AHRPam does not bind to the γC domain.

Even though chicken fibrinogen has an alanine residue at the amino terminus of its B-knob (AHRP-), a previously reported structure of chicken fibrinogen with bound GHRPam (and GPRPam) (*12*) showed the glycine-ending B-knob to be bound just as it is in human fibrin(ogen) fragments (*9*, *16*). Similarly, although the authentic B-knob in lamprey fibrinogen has the sequence GVRP-, fragments D and D-dimer from lamprey fibrinogen readily bind GHRP (*4*) and GHRPam (*31*, *32*), the latter peptide being shown by X-ray crystallography to bind in the very same manner that occurs in the mammalian holes.

It is important to keep in mind that the β- and γ-chains of vertebrate fibrinogen are homologous, implying that at one time in their history only a single kind of knob was bound by a single kind of hole (*33*). During its early evolution, fibrinogen differentiated to the point where there were two different knobs and two different holes, the two systems not necessarily having the same functions. It was long ago questioned whether the release of fibrinopeptide B exposes a polymerization site (*34*), and recent optical tweezer experiments have shown that A-knob−γC interactions alone account for the bulk of the forces holding the fibrin polymer together (*35*).

If we look back even further than the common ancestor of β- and γ-chains, it seems significant that the binding site for sialic acid in the homologous horseshoe crab protein tachylectin 5A (*36*) employs the exact same atoms in its backbone ridge, also exploiting the cis peptide bond that contributes to the binding site, underscoring the critical nature of this unusual and highly conserved feature.

Mutant Fibrinogens as a Guide to Function. Variant human fibrinogens reflect the different demands on the two kinds of knobs and holes. Thus, although a host of variants are known in which residues in the vicinity of the γC hole, including γGln329, γAsp330, and γAsp364, are mutated and cause clinical problems, none have been found for the equivalent residues in the βC hole (*37*), suggesting that the latter may be less critical. On the other hand, recombinant fibrinogens have been generated with substitutions at some of these β-chain positions, and in two of three cases, abnormalities in fibrin formed in vitro were observed (*38*).

As for genetic changes in the knobs, defective clotting has been found in persons who have substitutions among the first three positions of the fibrin A-knob (Gly-Pro-Arg), but the only variant known for the B-knob (Gly-His-Arg-) involves the amino-terminal glycine (*37*), a situation in which the abnormal behavior is more likely due to the negatively charged fibrinopeptide B not being properly released than to a defect in B-knob interaction, a subtle but important distinction that is often overlooked.

Nonetheless, there are some reported data to the contrary. Experiments with a recombinant fibrinogen in which residue βGly15 (destined to become the amino terminus of the B-knob) was changed to alanine showed that, although the thrombin-catalyzed release of fibrinopeptide B was slowed, it does occur at a measurable rate (*39*). Repolymerization of dispersed mutant fibrin lacking both fibrinopeptides was significantly less turbid than normal, arguing that the B-knob does play a role in fibrin formation and that an alanine residue at its amino terminus affects the process.

This observation notwithstanding, we nevertheless maintain that the role of the B-knob has changed during the course of evolution from one involved with polymerization to a less demanding one involving the duration of its existence (*8*). To wit, occupancy of the γC hole is critical for fibrin formation, but occupancy of the βC hole may be more important as a provocateur of fibrinolysis.

In summary, we have shown that the fibrin βC hole can bind alanine-ending peptides and the homologous γC hole does not. The distinction is attributed to a clash of the methyl group of the terminal alanine with a carboxyl group in the γ-chain that is essential to ligand binding. An equivalent carboxyl group in the β-chain is more flexibly disposed and able to accommodate the terminal alanine.

ACKNOWLEDGMENT

We thank Nick Nguyen at the University of California at San Diego X-ray facility and the staff at the Advanced Light Source at Lawrence Berkeley Laboratory for their assistance and cooperation. We are also grateful to Justin Kollman for assistance with some of the data collection, to Marcia Riley for preparing fibrinogen, to Justin Nand for help with computing and submitting material to the Protein Data Bank, and to Jessica Ng for help in preparing some illustrations.

SUPPORTING INFORMATION AVAILABLE

Contact residues at homologous positions in γ-chain and β-chain holes (Table S1), sequence alignment showing junctions split by thrombin and the A- and B-knobs that occur

in native fibrins (Figure S1), sequence alignments of the regions of fibrinogen β- and γ-chains that constitute the holes (Figure S2), electron density corresponding to the "lingering" calcium between the βC domain and the coiled coil (Figure S3), diagram of 14 putative hydrogen bonds observed between the A-knob and γC hole (Figure S4), diagram of 14 putative hydrogen bonds observed between the B-knob and βC hole (Figure S5), regions of FDGH complexed with GHRPam (Figure S6), structure of fragment D complexed with AHRPam (Figure S7), and hydrogen bonding that holds pivotal carboxyl groups of βD432 and γD364 in different positions in unoccupied β- and γ-holes (Figure S8). This material is available free of charge via the Internet at http://pubs.acs.org.

REFERENCES

1. Bailey, K., Bettelheim, F. R., Lorand, L., and Middlebrook, W. R. (1951) Action of thrombin in the clotting of fibrinogen, *Nature 167*, 233−234.
2. Doolittle, R. F. (1981) Fibrinogen and Fibrin, in *Thrombosis and Haemostasis* (Bloom, A. L., and Thomas, D. P., Eds.) pp 163−191, Churchill Livingstone, London.
3. Laudano, A. P., and Doolittle, R. F. (1978) Synthetic peptide derivatives that bind to fibrinogen and prevent the polymerization of fibrin monomers, *Proc. Natl. Acad. Sci. U.S.A. 75*, 3085−3089.
4. Laudano, A. P., and Doolittle, R. F. (1980) Studies on synthetic peptides that bind to fibrinogen and prevent fibrin polymerization. Structural requirements, number of binding sites and species differences, *Biochemistry 19*, 1013−1019.
5. Laudano, A. P., and Doolittle, R. F. (1981) Influence of calcium ion on the binding of fibrin amino-terminal peptides to fibrinogen, *Science 212*, 457−459.
6. Furlan, M., Rupp, C., Beck, E. A., and Scendsen, L. (1982) Effect of calcium and synthetic peptides on fibrin polymerization, *Thromb. Haemostasis 47*, 118−121.
7. Ferry, J. D., and Morrison, P. R. (1947) The conversion of human fibrinogen to fibrin under various conditions, *J. Am. Chem. Soc. 69*, 388−400.
8. Doolittle, R. F., and Pandi, L. (2006) Binding of synthetic B knobs to fibrinogen changes the character of fibrin and inhibits its ability to activate tissue plasminogen activator and its destruction by plasmin, *Biochemistry 45*, 2657−2667.
9. Everse, S. J., Spraggon, G., Veerapandian, L., Riley, M., and Doolittle, R. F. (1998) Crystal structure of fragment double-D from human fibrin with two different bound ligands, *Biochemistry 37*, 8637−8642.
10. Kostelansky, M., Betts, L., Gorkun, O. V., and Lord, S. T. (2002) 2.8 Å crystal structures of recombinant fibrinogen fragment D with and without two peptide ligands: GHRP binding to the "b" site disrupts its nearby calcium-binding site, *Biochemistry 41*, 12124−12132.
11. Weissbach, L., Oddoux, C., Procyk, R., and Grieninger, G. (1991) The β chain of chicken fibrinogen contains an atypical thrombin cleavage site, *Biochemistry 30*, 3290−3294.
12. Yang, Z., Kollman, J. M., Pandi, L., and Doolittle, R. F. (2001) Crystal structure of a native chicken fibrinogen at 2.7 Å resolution, *Biochemistry 40*, 12515−12523.
13. Hsieh, K. H. (1997) Localization of an effective fibrin b-chain polymerization site: Implications for the polymerization mechanism, *Biochemistry 36*, 9381−9387.
14. Everse, S. J., Pelletier, H., and Doolittle, R. F. (1995) Crystallization of fragment D from human fibrinogen, *Protein Sci. 4*, 1013−1016.
15. Spraggon, G., Everse, S. J., and Doolittle, R. F. (1997) Crystal structures of fragment D from human fibrinogen and its crosslinked counterpart from fibrin, *Nature 389*, 455−462.
16. Everse, S. J., Spraggon, G., Veerapandian, L., and Doolittle, R. F. (1999) Conformational changes in fragments D and double-D from human fibrin(ogen) upon binding the peptide ligand Gly-His-Arg-Pro-amide, *Biochemistry 38*, 2941−2946.
17. Merrifield, R. B. (1964) Solid phase peptide synthesis. 3. An improved synthesis of bradykinin, *Biochemistry 3*, 1385−1390.
18. Latallo, Z. S., Fletcher, A. P., Alkjaersig, N., and Sherry, S. (1962) Influence of pH, ionic strength, neutral ions, and thrombin on fibrin polymerization, *Am. J. Physiol. 202*, 675−680.
19. Otwinowski, Z., and Minor, W. (1997) Processing of X-ray diffraction data collected in oscillation mode, *Methods Enzymol. 276*, 307−326.
20. Collaborative Computational Project Number 4 (1994) A suite of programs for protein crystallography, *Acta Crystallogr. D50*, 760−763.
21. Brunger, A. T., et al (1998) Crystallography and NMR system: A new software suite for macromolecular structure determination, *Acta Crystallogr. D54*, 905−921.
22. Jones, T. A., Zou, J. Y., Cowan, S. W., and Kjeldgaard, M. (1991) Improved methods for building proteins in electron density maps and the location of errors in these models, *Acta Crystallogr. A47*, 110−119.
23. Berman, H. M., Westbrook, J., Feng, Z., Gilliland, G., Bhat, T. N., Weissig, H., Shindyalov, I. N., and Bourne, P. E. (2000) The Protein Data Bank, *Nucleic Acids Res. 28*, 235−242.
24. Brunger, A. T. (1992) *X-PLOR. Version 3.1, a system for X-ray crystallography and NMR*, Yale University Press, New Haven, CT.
25. Delano, W. L. (2002) *The PyMOL Molecular Graphics System*, DeLano Scientific, San Carlos, CA.
26. Pratt, K. P., Cote, H. C. F., Chung, D. W., et al. (1997) The primary fibrin polymerization pocket: Three-dimensional structure of a 30-kDa C-terminal γ chain fragment complexed with the peptide Gly-Pro-Arg-Pro, *Proc. Natl. Acad. Sci. U.S.A. 94*, 7176−7181.
27. Kyte, J. (2003) The basis of the hydrophobic effect, *Biophys. Chem. 100*, 193−203.
28. Yee, V. C., Pratt, K. P., Cote, H. C. F., LeTrong, I., Chung, D. W., Davie, E. W., Stenkamp, R. E., and Teller, D. C. (1997) Crystal structure of a 30 kDa C-terminal fragment from the γ chain of human fibrinogen, *Structure 5*, 125−138.
29. Burley, S. K., and Petsko, G. A. (1986) Amino-aromatic interactions in proteins, *FEBS Lett. 203*, 139−143.
30. Koshland, D. E. (1958) Application of a theory of enzyme specificity to protein synthesis, *Proc. Natl. Acad. Sci. U.S.A. 44*, 98−104.
31. Yang, Z., Spraggon, G., Pandi, L., Everse, S. J., Riley, M., and Doolittle, R. F. (2002) Crystal structure of fragment D from lamprey fibrinogen complexed with the peptide Gly-His-Arg-Pro-amide, *Biochemistry 41*, 10218−10224.
32. Yang, Z., Pandi, L., and Doolittle, R. F. (2002) The crystal structure of fragment double-D from cross-linked lamprey fibrin reveals isopeptide linkages across an unexpected D D interface, *Biochemistry 41*, 15610−15617.
33. Doolittle, R. F., Spraggon, G., and Everse, S. J. (1997) Evolution of vertebrate fibrin formation and the process of its dissolution, in *Plasminogen Related Growth Factors* (Bock, G. R., and Good, J. A., Eds.) CIBA Foundation Symposium 212, John Wiley & Sons, New York.
34. Hantgan, R., McDonagh, J., and Hermans, J. (1983) Fibrin assembly, *Ann. N.Y. Acad. Sci. 408*, 344−365.
35. Litvinov, R. J., Gorkun, O. V., Owen, S. F., Shuman, H., and Weisel, J. W. (2005) Polymerization of fibrin: Specificity, strength, and stability of knob-hole interactions studied at the single-molecule level, *Blood 106*, 2944−2951.
36. Karies, N., Beisel, H.-G., Fuentes-Prior, P., Tsuda, R., Muta, T., Iwanaga, S., Bode, W., Huber, R., and Kawabata, S. (2001) The 2.0-Å crystal structure of tachylectin 5A provides evidence for the common origin of the innate immunity and the blood coagulation systems, *Proc. Natl. Acad. Sci. U.S.A. 98*, 13519−13524.
37. Hauss, M., and Biot, F. (2000) A database for human fibrinogen variants, *Ann. N.Y. Acad. Sci. 936*, 89−90.
38. Kostelansky, M., Bolliger-Stucki, B., Betts, L., Gorkun, O. V., and Lord, S. T. (2004) Bβ Glu 397 and Bβ Asp398 but not Bβ Asp432 are required for " B:β" interactions, *Biochemistry 43*, 2465−2474.
39. Hirota-Kawadobora, M., Kani, S., Terasawa, F., Fujihara, N., Yamauchi, K., Tozuka, M., and Okumura, N. (2005) Functional analysis of recombinant Bβ15C and Bβ15A fibrinogens demonstrates that Bβ15G residue plays important roles in FBP release and in lateral aggregation of protofibrils, *J. Thromb. Haemostasis 3*, 893−890.

BI061219E